AN OBSERVATIONAL STUDY ON THERMAL ENVIRONMENT AND ENERGY CONSERVATION IN AN OFFICE BUILDING WITH MODERN CONVENIENCES

Hisaya Ishino[*1], Kimiko Kohri[*2], Koui Tsukamoto[*3], Keisuke Hirabayashi[*4]
[*1]Tokyo Metropolitan University, Tokyo + 192-0397 - Japan
[*2]Utsunomiya University, Utsunomiya + 321-8585 - Japan
[*3]Nihon Sekkei. Inc, Tokyo + 163-1329 - Japan
[*4]Shin Nippon Air Technologies Co. Ltd, Tokyo + 103-0021 - Japan

ABSTRACT

In this paper we report the findings of a survey conducted to evaluate the energy-conservation performance of an office building some time after construction, and present the results of a simulation that was performed to identify possible improvements to the building's cogeneration system. The indoor thermal environment was monitored over winter and summer, recording temperature and humidity variations and the vertical distribution of indoor air temperature. The simulation involved examining the effects of modified air-conditioning system operation, based on indoor humidity, ventilation temperature and survey data. The current energy-conservation performance of the cogeneration system is identified on the basis of the survey data, and suggested improvements for future operation based on the simulation results are proposed.

INTRODUCTION

In recent years, the number of buildings constructed using energy-saving designs has increased due to the increasing awareness of the benefits of energy conservation, both economic and environment. The recent rapid advances in computer technology have facilitated the development of energy-saving building designs by allowing detailed simulations, involving the incorporation of many energy-saving building techniques and features, to be conducted in the design stage. These techniques have been widely studied in terms of their design potential, however, there are very few studies concerning the actual post-construction performance of the design features and whether the overall building design does in fact provide significant energy savings. In this study, we examine the energy-conservation performance of an office building that was completed in May, 1999. The indoor environment was surveyed over two periods; winter (January 8 to February 13, 2000), and summer (July 20 to August 12, 2000). The parameters measured were indoor temperature (and vertical distribution), the operation of the air-conditioning system, and the energy-conservation performance of the cogeneration system. Based on these results, and the results of a simulation of this system, the optimum operation conditions for the heat source system and the air-conditioning system is clarified.

INDOOR THERMAL ENVIRONMENT

The survey was taken on the ninth floor of the building in question, and is assumed to be representative of the majority of floors in the building. The floor plan is shown in Fig. 1. The building has open faces on the northwest and southeast sides, and high-efficiency heat-reflecting double-glazed windows are installed with vertical-horizontal louvers on these two sides. These two perimeter areas are supplied with perimeter zone air conditioning to counter the skin load of these outward faces. One air conditioner is provided for each side, each with a paired-duct system for outdoor air load and internal heat load. The indoor thermal environment was measured in the NW perimeter zone and the NW interior zone. As a representative day for each survey period, the weather data for January 27 and July 31 are shown in Fig. 2. The variation in temperature and relative humidity in the interior zone is shown in Fig. 3 for the representative day.

The vertical distribution of temperature for the two zones of the building is shown in Fig. 4. The values are averaged over 30 minutes. There is virtually no vertical variation in temperature when the air-conditioning system is running (8:00 am to 8:00 pm) in either winter or summer in either zone. This is due to the fact that the paired-duct system provides a very high volume of air exchange, with the result that there the temperature difference between in the air-conditioning output and the ambient indoor temperature is very small. Furthermore, there is very little difference in temperature between the perimeter and interior zones, indicating that the perimeter zone air-conditioning design is very effective in intercepting heat transfer at the window boundary. In particular, in winter when cold drafts tend be generated at the window boundary, the effect of perimeter zone air conditioning is pronounced. Air conditioner load (NW perimeter zone) is shown in Fig. 5. The air conditioner is operated at a supply temperature of 28 °C in winter and 20 °C in summer. In addition, the air-conditioning system doesn't provide humidification and dehumidification.

In this building, in order to reduce the thermal conduction load and solar heat gain via the windows, high-efficiency heat-reflecting double-glazed windows are installed with vertical-horizontal louvers. The calculated reduction in load is shown in Fig. 6. The energy-saving configuration employed in the present building provides a 42.6% load reduction in winter and a 23.0% load reduction in summer compared to a standard system.

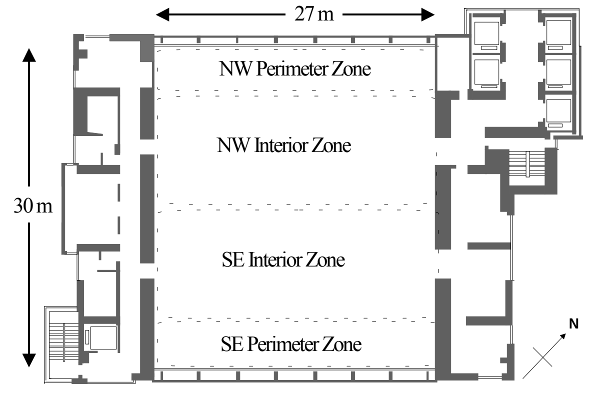

Fig. 1 Typical floor plan

Table 1 Building outline

Building use	Office building
Location	Tokyo
Total floor area	24,200 m^2
Number of stories	13 stories and 3 basements
Year of completion	May, 1999

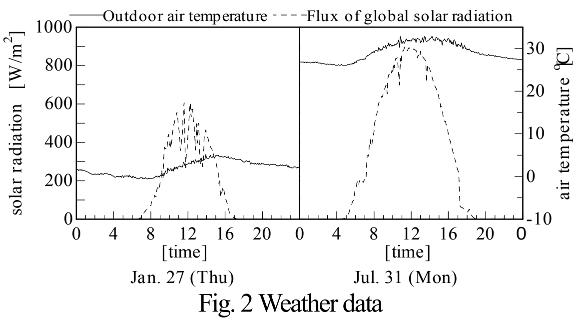

Fig. 2 Weather data

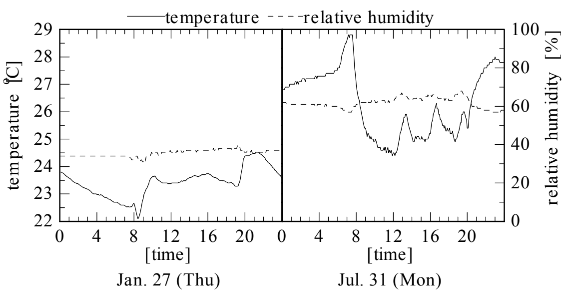

Fig. 3 Variation of temperature and humidity

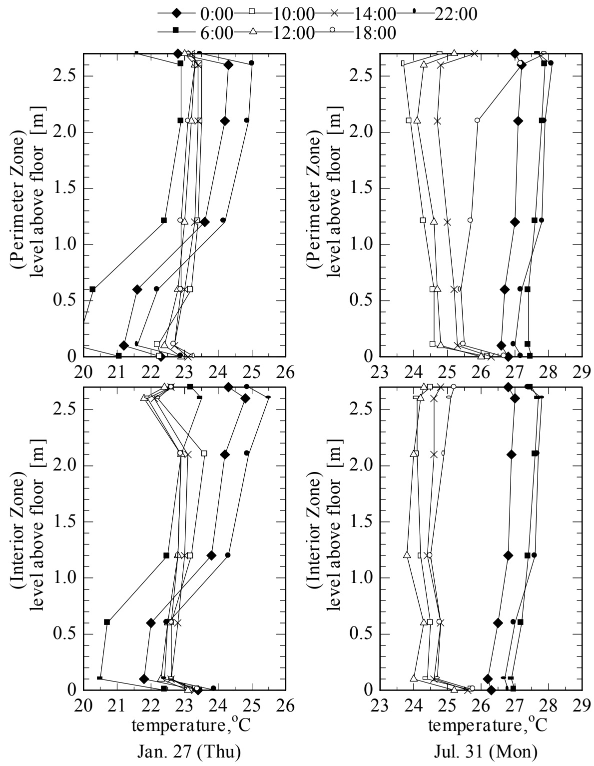

Fig. 4 Vertical distribution of temperature

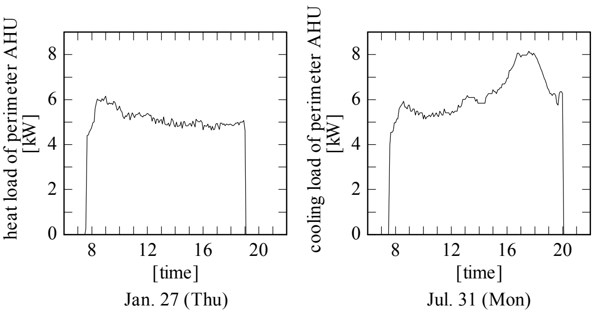

Fig. 5 Load of perimeter AHU

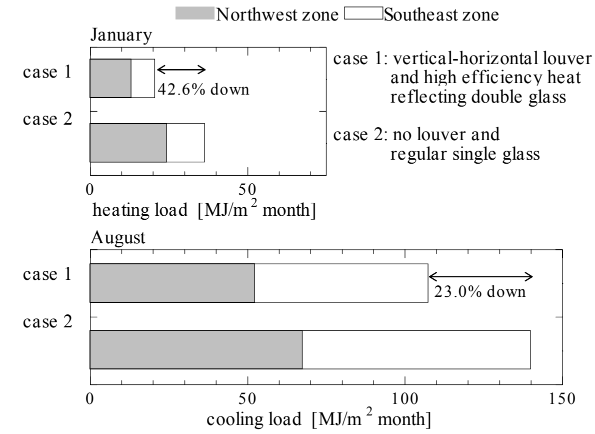

Fig. 6 Heat load saving rate by vertical-horizontal louvers and high-efficiency heat-reflecting double-glazed windows

OPERATIONAL CHARACTERISTICS OF AIR-CONDITIONING SYSTEM

A schematic of the air-conditioning system used in the present building (two per typical floor) is shown in Fig. 7. The paired-duct system consists of a constant air volume (CAV) system and a variable air volume (VAV) system. The CAV system provides cool or warm air after mixing a fixed quantity of fresh air with recycled internal air. The VAV system provides cool fresh air throughout the year. The operation of this paired-duct system with regard to supply air temperature and volume is important in realizing efficient climate control. In order to clarify the performance of the system under various conditions, we conducted a simulation in which the relationship between the preset temperature of supply and the indoor humidity was established.

Simulation

The basic data used for calculation is shown in Table 2, and the variation in internal thermal load for July 31 used as the model object is shown in Fig. 8. The simulation was based on the following assumptions:

1) The preset supply temperature is varied as follows in order to maintain the room temperature at 26 °C: If the room temperature falls below 26 °C, raise the VAV temperature. However, the VAV system does not provide heating. Therefore, raise the CAV temperature. If the room temperature exceeds 26 °C, reduce the VAV temperature (minimum 10 °C). If the required temperature is below 10 °C, reduce the VAV temperature to 10 °C and reduce the CAV temperature to the required temperature (no minimum).

2) Latent heat load is independent of humidity.

3) If dehumidification is active, the humidity of the cooling coil output is 95%.

Table 2 Basic data used for calculation

Floor area : 405 m^2, Room height : 2.7 m
Room temperature : 26 °C
Air volume of CAV : 1500 lit/sec (3.7 lit/sec m^2)
Maximum air volume of VAV : 1440 lit/sec (3.6 lit/sec m^2)
Minimum air volume rate of VAV : 20%
Volume of outdoor intake : 437.5 lit/sec (1.1 lit/sec m^2)

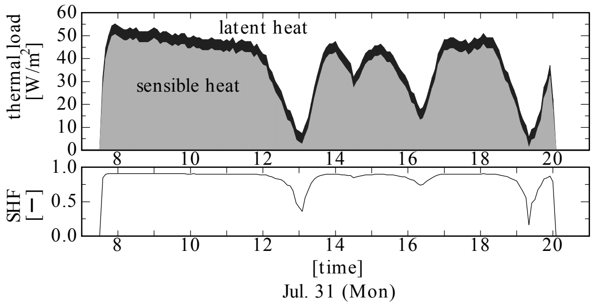

Fig. 8 Variation in internal thermal load for July 31

The simulation algorithm is explained below.

1) Check and change supply air temperature, and calculate VAV flow rate.

$q_{SCAV} = C_P \cdot \rho \cdot V_{CAV} (t_R - t_{CAVO})$

$q_{SVAV,min} = C_P \cdot \rho \cdot V_{VAV,min} (t_R - t_{VAVO})$

$q_{SVAV,max} = C_P \cdot \rho \cdot V_{VAV,max} (t_R - t_{VAVO})$

a) When $q_{SCAV} + q_{SVAV,min} \leq q_S \leq q_{SCAV} + q_{SVAV,max}$ (use preset supply air temperature).

$t_{CAV} = t_{CAVO}$, $t_{VAV} = t_{VAVO}$

$V_{VAV} = (q_S - q_{SCAV}) / \{ C_P \cdot \rho (t_R - t_{VAVO}) \}$

b) When $q_{SCAV} + q_{SVAV,min} > q_S$ (room temperature low).

$V_{VAV} = V_{VAV,min}$

$t_{VAV} = t_R - (q_S - q_{SCAV}) / (C_P \cdot \rho \cdot V_{VAV,min})$

When $t_{VAV} \leq t_R$, $t_{CAV} = t_{CAVO}$

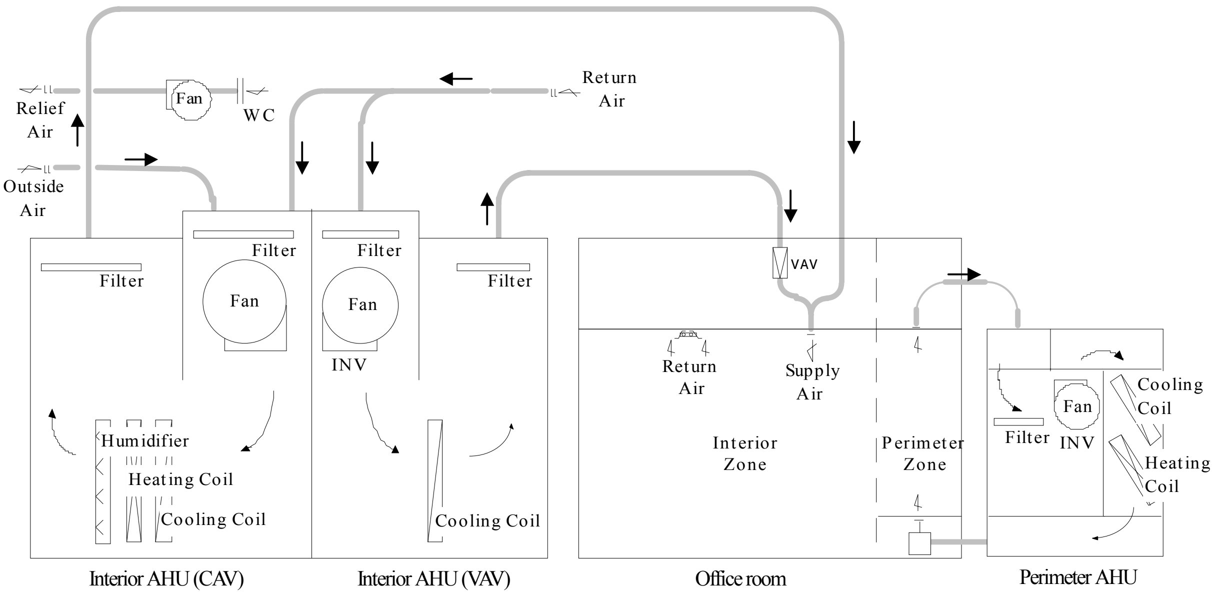

Fig. 7 Air conditioning system diagram (Typical floor)

When $t_{VAV} > t_R$, $t_{VAV} = t_R$, $t_{CAV} = t_R - q_S \ / (C_P \cdot \rho \cdot V_{CAV})$
c) When $q_{SCAV} + q_{SVAV,max} < q_S$ (room temperature high).
$V_{VAV} = V_{VAV,max}$
$t_{VAV} = t_R - (q_S - q_{SCAV}) / (C_P \cdot \rho \cdot V_{VAV,max})$
When $t_{VAV} \geq 10$°C, $t_{CAV} = t_{CAVO}$
When $t_{VAV} < 10$°C, $t_{VAV} = 10$
$q_{SVAV} = C_P \cdot \rho \cdot V_{VAV,max} (t_R - 10)$
$t_{CAV} = t_R - (q_S - q_{SVAV}) / (C_P \cdot \rho \cdot V_{CAV})$
2) Calculate temperature and sensible heat load.
$q_{SCAV} = C_P \cdot \rho \cdot V_{CAV} (t_R - t_{CAV})$
$q_{SVAV} = q_S - q_{SCAV}$
$t_D = k_{VAV} \cdot t_{VAV} + (1 - k_{VAV}) t_{CAV}$
  $k_{VAV} = V_{VAV} / V$
  $V = V_{CAV} + V_{VAV}$
$t_M = k_{OA} \cdot t_O + (1 - k_{OA}) t_R$
  $k_{OA} = V_{OA} / V_{CAV}$
$q_{SOA} = C_P \cdot \rho \cdot V_{OA} (t_O - t_R)$
$L_{SCAV} = q_{SCAV} + q_{SOA}$
$L_{SVAV} = q_{SVAV}$
3) Estimate the dehumidification state of the air conditioner, and calculate supply air humidity.
In the CAV system, if dehumidification is active, ICAV=1, otherwise ICAV=0. In the VAV system, if dehumidification is active, IVAV=1, otherwise IVAV=0.
a) Calculate supply air humidity if dehumidification is inactive in the CAV and the VAV system.
$q_{LCAV} = q_{LVAV} = 0$
$q_L + q_{LOA} = 0$
$q_L + r \cdot \rho \cdot V_{OA} (x_O - x_R) \cdot 10^{-3} = 0$
$\rightarrow x_R = x_O + q_L / (r \cdot \rho \cdot V_{OA} \cdot 10^{-3})$,
  $x_M = k_{OA} \cdot x_O + (1 - k_{OA}) x_R$
When $x_M \leq x95 (t_{CAV})$ and $x_R \leq x95 (t_{VAV})$, dehumidification is inactive.
$x_{VAV} = x_M$, ICAV = 0, $x_{VAV} = x_R$, IVAV = 0
When $x_M > x95 (t_{CAV})$ or $x_R > x95 (t_{VAV})$, dehumidification is active.
b) When $t_{CAV} \leq t_{VAV}$, CAV dehumidification is active.
$\rightarrow x_{CAV} = x95 (t_{CAV})$, ICAV = 1
A dehumidification judging of VAV air conditioner is as follows. If VAV dehumidification is inactive;
$q_{LVAV} = 0$
$q_L = q_{LCAV}$
$q_L = r \cdot \rho \cdot V_{CAV} (x_R - x_{CAV}) \cdot 10^{-3}$
$\rightarrow x_R = x_{CAV} + q_L / (r \cdot \rho \cdot V_{CAV} \cdot 10^{-3})$
When $x_R \leq x95 (t_{VAV})$, dehumidification is inactive.
$x_{VAV} = x_R$, IVAV = 0

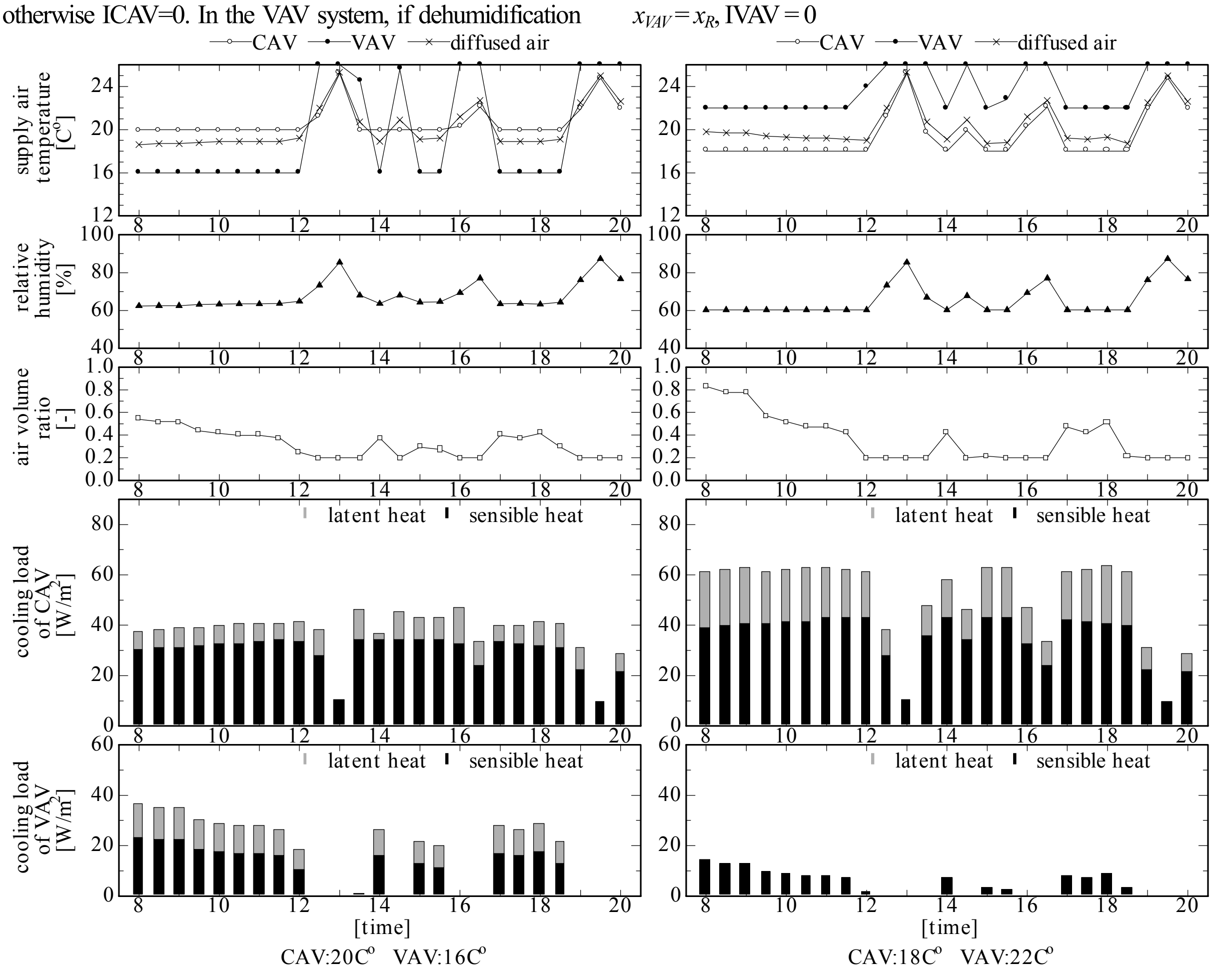

Fig. 9 Supply air preset temperature of air conditioner and indoor humidity environment

When $x_R > x95\,(t_{VAV})$, dehumidification is active.
$x_{VAV} = x95\,(t_{VAV})$, IVAV = 1
b´) When $t_{CAV} > t_{VAV}$, VAV dehumidification is active.
$\rightarrow x_{VAV} = x95\,(t_{VAV})$, IVAV = 1
A dehumidification judging of CAV air conditioner is as follows. If CAV dehumidification is inactive;

$$q_{LCAV} = r \cdot \rho \cdot V_{CAV}(x_R - x_M) \cdot 10^{-3} = r \cdot \rho \cdot V_{OA}\,(x_R - x_O) \cdot 10^{-3}$$

$$q_L = q_{LCAV} + q_{LVAV}$$

$$q_L = r \cdot \rho \cdot V_{OA}\,(x_R - x_O) \cdot 10^{-3} + r \cdot \rho \cdot V_{VAV}\,(x_R - x_{VAV}) \cdot 10^{-3}$$

$$\rightarrow x_R = x_{VAV} + (q_L + r \cdot \rho \cdot V_{OA} \cdot x_O \cdot 10^{-3} + r \cdot \rho \cdot V_{VAV} \cdot x_{OVAV} \cdot 10^{-3}) / \{ r \cdot \rho (V_{OA} + V_{VAV}) \}$$

$$x_M = k_{OA} \cdot x_O + (1 - k_{OA})\,x_R$$

When $x_M \leq x95\,(t_{CAV})$, dehumidification is inactive.
$\rightarrow x_{CAV} = x_M$, ICAV = 0
When $x_M > x95\,(t_{CAV})$, dehumidification is active.
$x_{CAV} = x95\,(t_{CAV})$, ICAV = 1
4) Calculation of humidity and latent heat.

$$x_D = k_{VAV} \cdot x_{VAV} + (1 - k_{VAV})\,x_{CAV}$$

$$k_{VAV} = V_{VAV} / V$$

$$x_R = x_D + q_L / (r \cdot \rho \cdot V)$$

$$x_M = k_{OA} \cdot x_O + (1 - k_{OA})\,x_R$$

$$q_{LCAV} = r \cdot \rho \cdot V_{CAV}\,(x_R - x_{CAV})$$

$$q_{LVAV} = r \cdot \rho \cdot V_{VAV}\,(x_R - x_{VAV})$$

$$q_{LOA} = r \cdot \rho \cdot V_{OA}\,(x_O - x_R)$$

$$L_{LCAV} = q_{LCAV} + q_{LOA}$$

$$L_{LVAV} = q_{LVAV}$$

Result of simulation

The results for initial temperature settings of 16 °C VAV 20 °C CAV are shown in Fig. 9. Except for the short periods when the cooling load becomes very small, the supply air temperature remains at the initial setting and the indoor relative humidity is constant at 60%. A setup of VAV system remains as it is, and if it lowers the setting supply air temperature of CAV system further, it can lower indoor relative humidity to 60% or less. However, if the supply air temperature in the CAV system is lower, in order to reduce the amount of ventilation in the VAV system, the volume of air exchange decreases. If the initial settings are 18 °C CAV and 22 °C VAV (Fig. 9), the cooling load of the VAV system becomes all sensible heat, and all latent heat loads and the remaining sensible heat are processed by the CAV system. Compared with the previous case (16 °C VAV, 20 °C CAV), although indoor relative humidity is similar, a greater volume of VAV ventilation is required to achieve that level. Here we used the survey data for simulation, however in actual design it is possible to simulate a wide range of operating conditions.

ENERGY-CONSERVATION PERFORMANCE OF COGENERATION SYTEM

A schematic of the cogeneration system (CGS) used in the present building is shown in Fig. 10. The CGS is powered by a lean 300 kW gas combustion engine; all generating electricity is used in this building and the exhaust heat is used for cooling, heating and hot water supply. To convert this exhaust heat into cooling energy, conventionally, application-specific hot-water driven and single stage absorption refrigeration machines were required. However, newly developed direct-fired gas absorption chilled and hot water generator has succeeded such systems, resulting in not only space and energy savings, but also in improved system operability. For heating, water from a hot water return header is directly heated by the heat exchanger. The rest of exhaust heat is used for warming domestic hot-water. The operation of the CGS in this building was still in the first year at the time of this survey, and as such neither control nor flux adjustment were perfect, the problem of adjustment of a measurement range and error of a measuring instrument and the operator may not be experienced with the system. By determining the current operating conditions and energy-conservation performance of the CGS and identifying the areas that require improvement, we will be able to suggest optimum operating conditions for realizing further energy savings.

The CGS is operated at the rated output for 14 hours, between 8:00 am and 10:00 pm, every weekday. As shown in Fig. 11, although the power load in August is greater than in December, as the CGS is performing rated operation, the amount of power generation is stable at about 4 MWh in both August and December. The heat load per day in August is about 80 GJ, with a much lower heat load in December (30 GJ). The heat power ratio in August exceeded 1.0 during the week, whereas the same ratio was about 0.5 in December. The utilization ratio for waste heat is higher in December than in August due to the higher efficiency of using waste heat for heating (as opposed to cooling). The energy saving ratio is 0.5% to 3.0% in December and in August by using waste heat. The amount of gas saving is in turn greatly affected by the cooling load factor of the direct-fired gas absorption chilled and hot water generator. The cooling load factor and gas saving for the most expensive (August 18) and least expensive (August 30) weekdays in summer are shown in Fig. 12. The gas saving on August 18 is approximately 30 N m^3/h, compared to 20Nm^3/h on the 30th. As the characteristic for which the amount of waste heat utilization

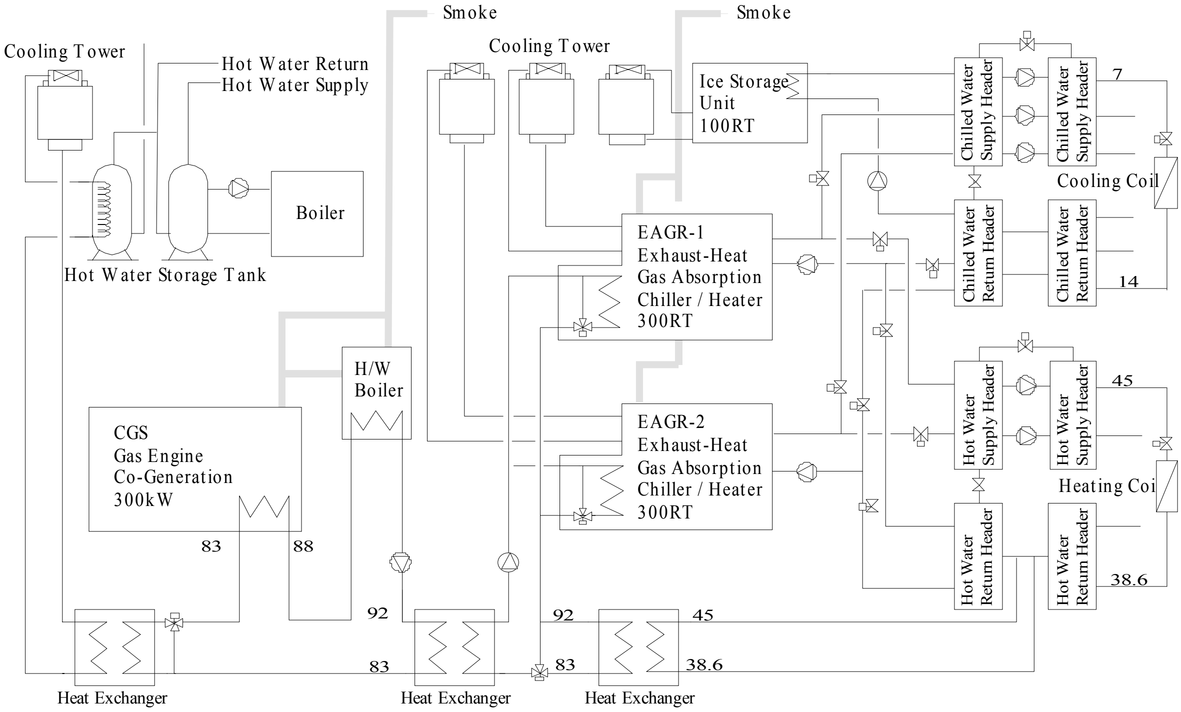

Fig. 10 Heating / cooling plant system diagram

increases most is the operation of the direct-fired gas absorption chilled and hot water generator when the cooling load factor is over or below 50%, the gas saving on the 18th is greater than that on the 30th. This demonstrates that high cooling load does not necessarily mean a greater utilization of waste heat. At the time of heating, in order to heat directly by the heat exchanger, if heating load is large, the amount of waste heat utilization will also increase.

The amount of waste heat utilization at the time of cooling is determined by the cooling load factor of the chilled and hot water generator. Then, if we calculate the amount of waste heat utilization from the cooling load factor, it is possible to simulate the amount of primary energy in case of heat oriented operation. The conditions of calculation are as follows:

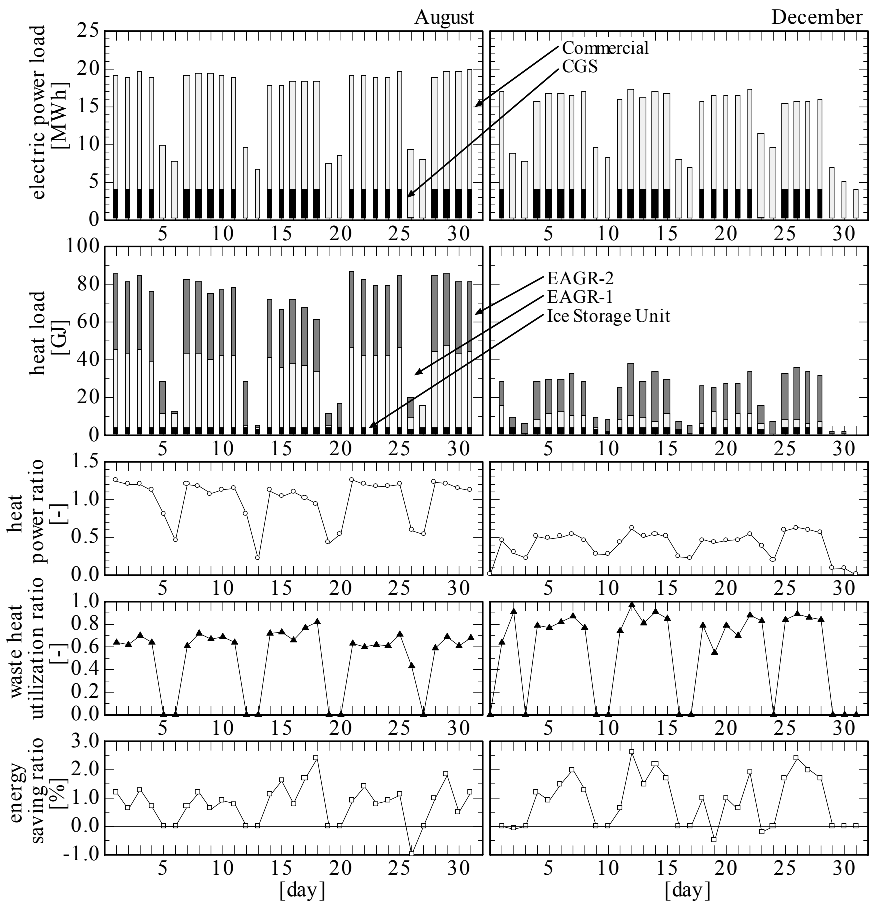

Fig. 11 Operational characteristic of CGS

1) The output of the gas engine dynamo is set to 75kW or more. The waste heat generated under these conditions is 528.8 MJ/h.

2) The heat recovery water temperature is assumed to be a constant 88 °C.

3) The output of the dynamo is increased to 150 kW after 1 hour of operation. The waste heat generated under these conditions is 693.3 MJ/h.

4) The amount of maximum waste heat recovery per a chilled and hot water generator is set to 575.3 MJ/h.

The calculation results for the primary energy consumption and energy conservation ratio in August are shown in Table 3. CASE-A is without the recovery of waste heat, CASE-B is the current conditions of recovery (from survey data), and CASE-C is for the modified operation of the gas engine. Although energy savings are certainly realized in CASE-B, this saving can be doubled by modifying the operation of the gas engine to that of CASE-C.

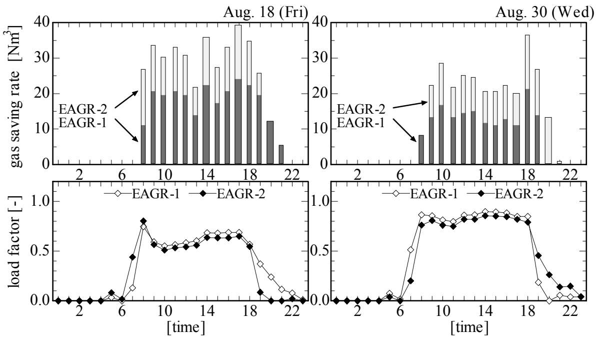

Fig. 12 Cooling load factor and gas saving rate

Table 3 Primary energy consumption and energy conservation ratio

	Electricity	Gas	Total	Energy Conservation Ratio
	[GJ/month]	[GJ/month]	[GJ/month]	[%]
CASE-A	5093.6	1960.0	7053.6	-
CASE-B	4204.6	2782.0	6986.7	0.95
CASE-C	4341.4	2566.1	6907.6	2.07

Primary energy equivalent value Electricity : 10.25 [MJ/kWh]
Gas : 46.1 [MJ/Nm^3]

CONCLUSION

In this study we examined the energy-conservation performance of an office building fitted with a cogeneration system and various energy-saving features. A simulation of the effects of varying a number of system parameters was conducted, and the results helped to clarify the present conditions of operation, and allowed us to propose improvements to the operation of the system. The findings of the study can be summarized as follows:

The cold draft generated at the window boundary in winter is successfully prevented by the installation of perimeter zone air conditioning.

Although the paired duct system employed allows the indoor relative humidity to become a little high in summer, it has the merit that a high volume of air is exchanged, increasing the quality of indoor air.

As a result of the high volume of air exchange, the temperature difference between supply air and ambient indoor air is very small, and as such there is almost no vertical difference in indoor temperature.

Although the CGS is provides significant energy savings when the heat load in summer and winter is large, an important consideration is whether the CGS is energy efficient in the transition seasons when heat load becomes small. In this case, it is necessary to collect further data for other times of the year in order to propose operating conditions that will provide optimum energy savings throughout the year.

ACKNOWLEDGEMENTS

The authors wishes to acknowledge the support of Nobuaki Ohsato of Amway Japan Limited and Masahiro Ogasawara of Nihon Sekkei. Inc.

NOMENCLATURE

q_S	room sensible cooling load [W/m^2]
q_{SCAV}	room sensible cooling load in CAV air conditioner [W/m^2]
q_{SVAV}	room sensible cooling load in VAV air conditioner [W/m^2]
V_{CAV}	supply air volume in CAV air conditioner [lit/sec m^2]
V_{VAV}	supply air volume in VAV air conditioner [lit/sec m^2]
V	total supply air volume [lit/sec m^2]
k_{VAV}	air volume rate of VAV air conditioner [lit/sec m^2]
t_R	room temperature [°C]
t_D	diffused air temperature [°C]
t_{CAV}	supply air temperature in CAV air conditioner [°C]
t_{VAV}	supply air temperature in VAV air conditioner [°C]
C_p	specific heat of air (=1.0) [J/g K]
ρ	density of air (=1.2) [g/lit]
q_L	room latent cooling load [W/m^2]
q_{LCAV}	room latent cooling load in CAV air conditioner [W/m^2]
q_{LVAV}	room latent cooling load in VAV air conditioner [W/m^2]
x_R	room absolute humidity [g/g]
x_D	diffused air absolute humidity [g/g]
x_{CAV}	supply air absolute humidity in CAV air conditioner [g/g]
x_{VAV}	supply air absolute humidity in VAV air conditioner [g/g]
r	heat of vaporization of water (=2500) [J/g]

L_{SCAV} CAV air conditioner sensible cooling load [W/m^2]
L_{SVAV} VAV air conditioner sensible cooling load [W/m^2]
L_{LCAV} CAV air conditioner latent cooling load [W/m^2]
L_{LVAV} VAV air conditioner latent cooling load [W/m^2]
q_{SOA} outdoor air sensible cooling load [W/m^2]
q_{LOA} outdoor air latent cooling load [W/m^2]
V_{OA} volume of outdoor air intake [W/m^2]
t_O outdoor air temperature [°C]
t_M mixing air temperature [°C]
x_O outdoor air absolute humidity [g/g]
x_M mixing air absolute humidity [g/g]